Gaining insight into regional coastal changes on La Réunion island through a Bayesian data mining approach

Thomas Bulteau, Audrey Baills, Lise Petitjean, Manuel Garcin, Hindumathi Palanisamy, Gonéri Le Cozannet

Geomorphology 228 (2015) 134–146

Contents lists available at ScienceDirect

Geomorphology

journal homepage: www.elsevier.com/locate/geomorph

Gaining insight into regional coastal changes on La Réunion island through a Bayesian data mining approach

T. Bulteau [a,*], A. Bailles [a], L. Petitjean [a,b], M. Garcin [a], H. Palanisamy [c], G. Le Cozannet [a]

[a] BRGM, 3 avenue Claude Guillemin, 45000 Orléans, France
[b] Laboratoire de Météorologie Dynamique, Paris, France
[c] LEGOS, Toulouse, France

ARTICLE INFO

Article history:
Received 12 February 2014
Received in revised form 28 August 2014
Accepted 1 September 2014
Available online 16 September 2014

Keywords:
Shoreline changes
Bayesian networks
Sea-level rise
Vertical ground motions
Coastal databases
La Réunion island

ABSTRACT

Recent works have highlighted the interest in coastal geographical databases – collected for coastal management purposes – for obtaining insight into current shoreline changes. On La Réunion, a tropical volcanic high island located in the Southern Indian Ocean, a dataset is available which describes shoreline changes, the coastal geomorphology and the presence of anthropic structures. This database is first supplemented with information on the exposure of each coastal segment to energetic waves and to estuarine sediment inputs. To incorporate relative sea-level changes along the coast in the database, levelling data are analysed in combination with GPS, satellite altimetry and sea-level reconstructions. Finally, a method based on Bayesian networks is used to assess the probabilistic relationships between the variables in the database. The results highlight the high degree of dependency between variables: a retrospective model is able to reproduce 81% of the observations of shoreline mobility. Importantly, we report coastal ground motions for La Réunion island of the order of 1 to 2 mm/year along the coast. However, the resulting differing rates of relative sea-level rise do not significantly impact on shoreline changes. Instead, the results suggest a major control of geological processes and local coastal geomorphic settings on shoreline evolution. While any exploration of a coastal database needs to be complemented with human reasoning to interpret the results in terms of physical processes, this study highlights the significance of revisiting other datasets to gain insight into coastal processes and factors causing shoreline changes, including sea-level changes.

1. Introduction

Individual processes that cause shoreline mobility are well known and result from the impacts of hydrometeorological factors, anthropogenic actions and biological processes on sediment stocks inherited from previous states of the coastal system. These processes and their interactions at various spatial and temporal scales are highly complex, so that understanding the respective roles of each factor in controlling shoreline mobility remains a real challenge. In the last two decades, local coastal observations have been increasingly gathered into large coastal datasets (Quelennec et al., 1998; Thieler and Hammar-Klose, 1999; Eurosion, 2004; Yin et al., 2012) in order to inform regional coastal management and to anticipate future changes. Incidentally, such databases have also been used to improve our understanding of recent coastal evolution and the associated causes (Hapke and Plant, 2010; Gutierrez et al., 2011; Yates and Le Cozannet, 2012). Large coastal databases contain – at least partially – information on shoreline mobility, coastal geomorphological settings and forcing factors. By exploring these coastal databases through data mining approaches, it becomes possible to examine the statistical relationships relating these variables.

Among existing data mining approaches, Bayesian networks (BNs) have become a very popular tool since the early '90s (Heckerman, 1997; Aguilera et al., 2011). A BN is a graphical model that encodes probabilistic relationships between variables of interest. They have been used in a variety of different applications, ranging from artificial intelligence to environmental modelling or as decision-support tools (Berger, 2000; Uusitalo, 2007; Catenacci and Giupponi, 2013).

Along with other systemic approaches such as Boolean models (Karunarathna and Reeve, 2007, 2008), the BN approach has been used to model physical coastal processes (Hapke and Plant, 2010; Gutierrez et al., 2011; Plant and Holland, 2011a,b; Plant and Stockdon, 2012; Yates and Le Cozannet, 2012; Loureiro et al., 2013). In these studies, the relationships between shoreline mobility and other coastal geomorphological settings and forcing factors are modelled as Bayesian networks. Applied to coastal databases on the eastern coast of the USA (Gutierrez et al., 2011) this approach suggested that relatively moderate differences in the rates of sea-level rise along this coast (a few mm/year) are an important cause for the different rates of shoreline erosion in this area (a result already suggested by Zhang et al., 2004). However, it

* Corresponding author. Tel.: +33 238643945.
E-mail address: t.bulteau@brgm.fr (T. Bulteau).

http://dx.doi.org/10.1016/j.geomorph.2014.09.002

remains unclear whether this conclusion can be generalized to other coastal sites (Cazenave and Le Cozannet, 2014). To confirm such results, it is necessary to explore other coastal datasets in order to check whether these relationships between sea-level rise and shoreline erosion are fortuitous, related to local conditions or if they apply to many coasts around the world.

The coastal dataset for La Réunion island (Southern Indian Ocean; De La Torre, 2004) was initially compiled for coastal management purposes, in order to characterize and map the coastal morphology and morphodynamics of the island and anticipate future trends (Le Cozannet et al., 2013). For each coastal segment, this dataset describes the observed multidecadal shoreline mobility, geomorphic settings and the presence of anthropic structures in the vicinity of the segment. In this study, we first complete this coastal dataset by constructing three other variables, namely the exposure to energetic waves, the presence of an estuary and the rate of relative sea-level rise, then, we use the method proposed by Gutierrez et al. (2011) to quantify the strength of known relationships between the variables. This enables one to identify the main factors driving decadal shoreline mobility in La Réunion while revealing the particular role of the rate of relative sea-level rise in coastal evolution.

The paper is organized as follows: in part 2, the theory of the BN approach and the tools used to evaluate the BN performance are briefly presented; in part 3, the study site and the dataset used are described; part 4 presents the results (relative sea-level changes at the coast and assessment of the BN performance); and part 5 examines to which extent the results can be interpreted in terms of physical processes.

2. Bayesian networks and their application for exploring coastal databases

A BN is a tool to graphically represent knowledge about a given system and to compute dependencies between parts of that system in terms of probabilities (Pearl, 1986). Formally, a BN $\mathscr{B} = (\mathcal{G}, \theta)$ is defined by:

- A directed acyclic graph $\mathcal{G} = (X,\mathrm{E})$, E being the set of directed edges representing causal relationships between the nodes of the graph that represent a set of random variables $X = \{X_1, \ldots, X_n\}$,
- Parameters $\theta = \{P(X_i|Pa(X_i))\}_{i = 1..\ n}$ that depict the conditional probability of each node X_i given its parents $Pa(X_i)$ within $\mathcal{G}$.

While $\mathcal{G}$ describes qualitatively the dependence (or independence) between variables, θ provides a more quantitative insight. In addition, the conditional independencies expressed by $\mathcal{G}$ allow simplification of the joint probability distribution of X into a product of local conditional probabilities which depend only on the considered node and its parents (see e.g. Pearl, 1986):

$$P(X_1, \ldots, X_n) = \prod_{i=1}^{n} P(X_i|Pa(X_i)) = \prod_{i=1}^{n} \theta_i. \quad (1)$$

This formula is a fundamental property of BNs. It is used for inference that is to compute the probability of any random variable X_i from observations of the others.

Hapke and Plant (2010) and Gutierrez et al. (2011) proposed a BN-based approach to explore coastal databases. The first step in their approach consists of defining a network structure $\mathcal{G}$, formalizing a qualitative understanding of coastal systems. Therefore, $\mathcal{G}$ displays the relationships between a few important parameters of a coastal database such as, for example: geomorphology, wave climate, tidal range, decadal sea-level changes and shoreline evolution. Importantly, in order to be used in a BN, the coastal variables must have states that are mutually exclusive and collectively exhaustive (Heckerman, 1997), which implies simplifying and harmonizing the raw coastal observations, like, for example, considering only a limited number of coastal geomorphology classes (cliffs, wetlands, beaches…) out of the numerous existing ones (Finkl, 2004).

In a second step, the parameters θ are computed from the database (learning phase). When a complete dataset (i.e. no missing data) is considered, the learning phase is straightforward: the parameters θ are determined using the maximum likelihood approach, which consists in estimating the probability of an event with its frequency of appearance in the dataset (Naïm et al., 2007).

The next step of the approach consists of creating a predictive model for shoreline mobility. The conditional probability distribution of shoreline mobility is written as:

$$P\left(SM^i \middle| \widetilde{X}_j\right), \forall i \quad (2)$$

where SM^i is the ith discretized state of the shoreline mobility variable and $\widetilde{X}_j$ represents a combination of all the other variables. For a given combination $\widetilde{X}_j$, the predicted shoreline mobility is the mode of the conditional probability distribution (2). This is written as:

$$SM_{pred} = \arg\max_i \left(P\left(SM^i \middle| \widetilde{X}_j\right)\right) \quad (3)$$

The probability value gives an indication of the prediction uncertainty. Assessing to which extent the observed shoreline mobility can be correctly predicted helps us evaluate the relevance and efficiency of our BN to represent the coastal system. As the same data were used for inference and learning, we are in a case of 'overfitting' (Aguilera et al., 2011) and the resulting predictions might be biased. However, the Bayesian model here is not used to predict future states of coastal geomorphology but as a data mining technique to analyse the relationships between the variables in the database.

The last step consists of analysing what are the most discriminating variables with respect to shoreline changes. This is done by evaluating the BN performance through statistical tools, such as the log-likelihood ratio (LR) which evaluates how much the knowledge of shoreline mobility has been improved owing to the other observations. For a given coastal segment (k) the LR is defined as follows:

$$LR_{(k)} = \log\left(P\left(SM_{(k)} \middle| O_{(k)}\right)\right) - \log\left(P\left(SM_{(k)}\right)\right) \quad (4)$$

where $SM_{(k)}$ is the observed shoreline mobility of segment (k) and $O_{(k)}$ represents the set of all the other variable states corresponding to segment (k).

The $LR_{(k)}$ can be summed over all coastal segments to give a global score of the model performance. By comparing how the global LR evolves with the number and type of variables, Gutierrez et al. (2011) evaluate the relative importance of each variable of the model with respect to shoreline changes.

In this paper, the same method is applied to another dataset for La Réunion island. However, in this application, because each coastal segment has a different length, the learning phase of the network is modified in a way that the importance of each segment is evaluated according to its length. In other words, each coastal segment does not count for one observation during the learning phase; its own length is used instead to weight it in the computation of the maximum likelihood estimators of parameters θ. Subsequently, the global score of LR is also computed accounting for the respective lengths of the segments:

$$LR = \frac{1}{total\ \ length} \sum_k LR_{(k)} length_{(k)}. \quad (5)$$

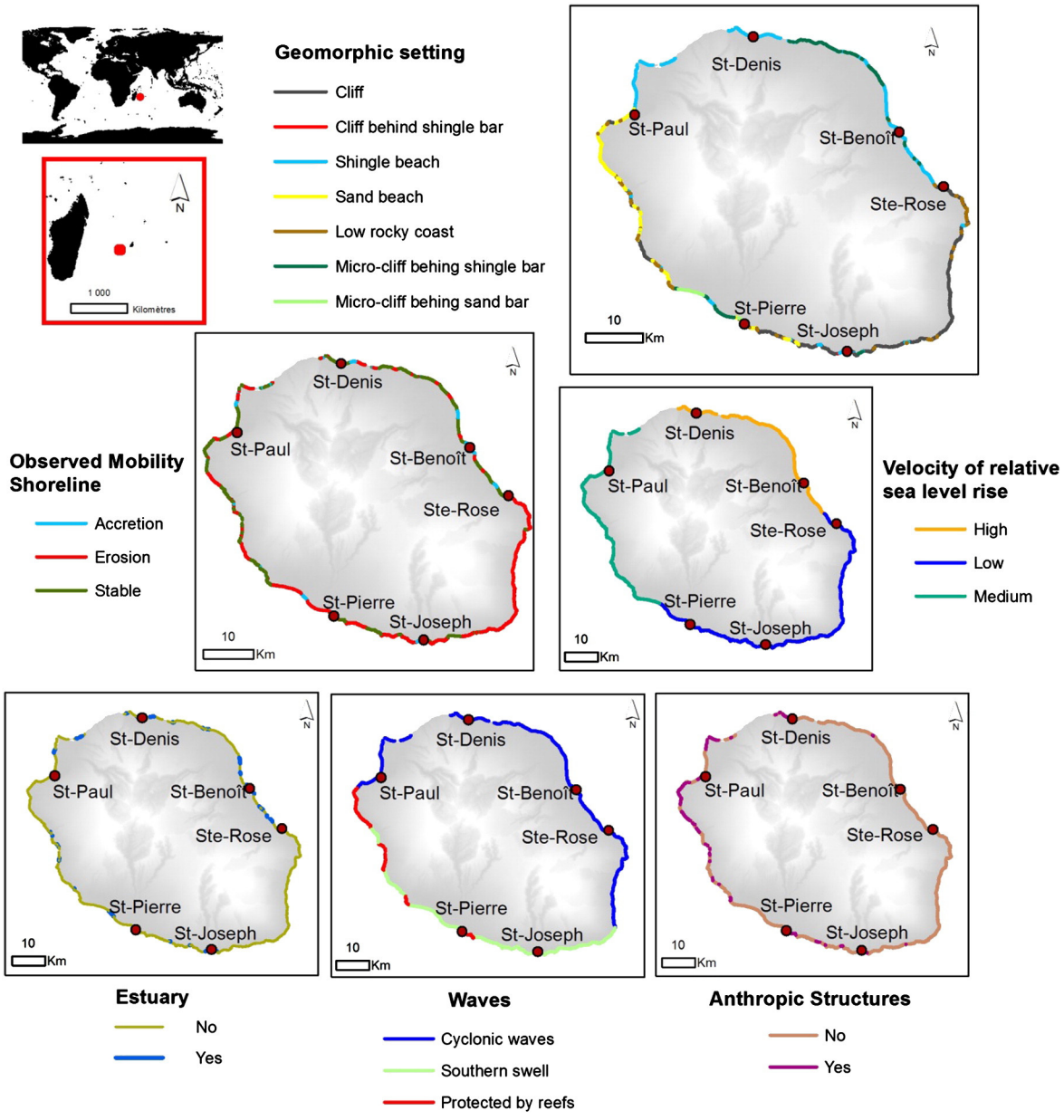

Fig. 1. Location of La Réunion island in the southwest Indian Ocean and spatial representation of the 6 variables of our coastal dataset. Some coastal sectors are completely artificial (e.g. coastal road located west from St-Denis) and cannot be described by the geomorphic settings represented in the top right image. These sectors are not considered in this study. Conversely, coastal segments to which a geomorphic setting can be assigned and where some anthropic structures exist (e.g. walls, etc.) are shown in the bottom right map.

3. Study site and data

3.1. Geographical and geological context

La Réunion is a French volcanic island located in the Western Indian ocean in the Mascarene archipelago (55°30′ E, 21° S), about 700 km east of Madagascar (Fig. 1). The island is made of two volcanoes, products of a hotspot activity. The oldest volcano (Piton des Neiges) caused the formation of the island 3 million years ago and has been inactive for the last 12,000 years (Rocher, 1988). It is located north-west of the island and culminates at 3070 m. The second volcano, the Piton de la Fournaise, is more recent (500,000 years old, Gillot and Nativel, 1989) and is currently one of the most active volcanoes on Earth. It reaches an altitude of 2621 m and is located south-east of the island. The emerged part of the island (about 2512 km^2) represents only 3% of the whole geological formation, which rises from the ocean floor at 4000 m depth. Soil erosion processes have shaped this volcanic formation, creating contrasting reliefs.

The shoreline is 250 km long and is made of a locally scoriaceous basaltic rocky coast. It is sometimes covered by surficial formations after weathering of the substratum and remodelling of slopes (e.g. mudslides, debris avalanches). The island has also a dense hydrographical network which supplies pebble and sand to the shores. In the west of the island, coral reefs have developed protecting beaches from direct wave impacts and supplying them with detrital organic materials. The reefs are relatively narrow (maximum extent from the shore 520 m) and form a discontinuous belt (Fig. 1). Cliffs and low rocky coasts represent about 42% of the whole shoreline whereas almost 45% is made up of beaches. The remaining 13% are completely artificial parts of the coast (De La Torre, 2004).

Table 1
Description of the initial (De La Torre, 2004) and final states of the variables.

Variable	Initial	Final
Morphotype (initial)/Geomorphic setting (GS) (final)	Coherent cliff Low rocky coast Loose or mixed cliff Loose or mixed micro-cliff Riverine shingle bar Marine shingle bar Basaltic sand beach Basaltic sand dune Unevolved coral mixed sand beach Unevolved coral biodetrital sand beach Evolved coral biodetrital sand beach	1-Cliff 2-Cliff behind shingle bar 3-Low rocky coast 4-Micro-cliff behind shingle bar 5-Micro-cliff behind sand bar 6-Shingle beach 7-Sand beach
Anthropic structure (AS)	Completely artificialized Partially artificialized No	1-Yes (corresponding to Partially artificialized state) 2-No
Shoreline mobility (SM)	Stability In transition Moderate erosion Severe erosion Accretion	1-Stability (combining Stability and In transition states) 2-Erosion (combining Moderate erosion and Severe erosion states) 3-Accretion
Estuary	N/A	1-Yes 2-No
Exposure to energetic waves (Waves)	N/A	1-Mainly exposed to cyclonic waves 2-Mainly exposed to southern swells 3-Protected by reefs
Velocity of relative sea level rise (RSLR)	N/A	1-High 2-Low 3-Medium

3.2. Description of the coastal database

3.2.1. Database as a whole

The coastal database for La Réunion island is based on a GIS (Geographical Information System) dataset compiled by the French Geological Survey (BRGM) from field campaigns undertaken between March and June 2004 (De La Torre, 2004), which were updated using more recent information on coastal processes and harmonized to make it suitable for use within a BN approach.

The initial database comprised three variables (Table 1): morphotype (11 states), the presence of anthropic structures (3 states) and shoreline mobility (5 states), that divided the coastline into segments with homogeneous characteristics. This dataset cannot be readily explored using a Bayesian network: for example, the geomorphic setting of a given coastal segment could be described with a combination of 2 morphotypes (e.g. coherent cliff plus marine shingle bar). This counters to the rule of mutually exclusive and collectively exhaustive states for BN variables (Heckerman, 1997). Hence, new classes were defined that both comply with this rule and adequately represent the coastal geomorphology in the island. Another point to consider when preparing the database is as follows: the more states per variable and the more complicated the model structure, the more data is needed to efficiently capture complex empirical distributions (Myllymäki et al., 2002; Uusitalo, 2007). Here, observations are limited by the island shoreline length. Thus, the number of states was reduced to a minimum while maintaining a satisfying representation of the coastal system: from the initial numbers of states of morphotype, anthropic structures and shoreline mobility, we settled on only 7 geomorphic settings, 2 states for the presence of anthropic structures and 3 states of shoreline mobility.

The states of the simplified variables are presented in Table 1. This table also shows that to complete the description of the coastal system, three new variables were added — exposure to energetic waves (3 states) (adapted from Lecacheux et al., 2012), presence of an estuary (2 states) (created within the present study), and the rate of relative sea-level rise (3 states) (created within the present study). Detailed information on the different variables is given in the following subsections. Fig. 1 presents the final coastal data used in the next steps of the approach. The final database divides the island's coastline into 384 segments with different lengths.

3.2.2. Shoreline evolution

The shoreline evolution dataset is based on extensive field observations of shoreline change indicators, such as micro-cliff, apparent tree roots at the upper beach, beach slopes, traces of fallen rocks at the top of the cliff, the presence of an upper beach berm, a small delta, a shingle bar at the foot of the cliff, vegetation of backshore or dunes. De La Torre (2004) positively compared his interpretation from field observations with aerial photographs from IGN campaigns of 1966, 1978 and orthophotographs of 1997. Although this period covers the intense economic and demographic development of the island, several significant climatic events (cyclones Hyacinthe (1980), Florine (1981), Clotilda (1987), Firinga (1989), Colina (1993), Hollanda (1994), Dina (2002)…) as well as volcanic events (eruptions of the Piton de la Fournaise reaching the sea in 1977 and 1986), the good agreement between the two approaches suggests that the coastal dataset can be interpreted as an indication of the main trends of coastal mobility over the last three decades.

3.2.3. Coastal geomorphology, human actions, inputs from river sediments to the coast

In addition to the shoreline evolution, the coastal dataset collected by De La Torre (2004) includes a description of the geomorphic setting for each coastal segment, as well as information about potential anthropic structures in the vicinity of the segment (a wall at the upper beach, a ramp for boats on a shingle beach, homes on top of micro-cliffs or directly on the beach, tourism facilities such as coastal promenades or artificial saltwater swimming pools, jetties, etc.) (Fig. 1). All these anthropic structures can potentially affect shoreline mobility (Eurosion, 2004) by disrupting the alongshore sedimentary transport (e.g. jetty at Saint-Benoît), the sediment transfer from rivers (e.g. river d'Abord at Saint-Pierre) or between sand dunes and beaches (e.g. Etang-Salé les bains), or by modifying the local wave regime (e.g. homes at Saint-Pierre located on the seafront). Thus, they can favour erosion but they can also locally protect the shoreline from it (e.g. a jetty can favour accretion upstream of the alongshore drift, an artificial swimming pool can protect a beach from the erosive action of waves, as has been observed at the Grande Anse beach.). Coastal segments that are completely artificial are discarded from the dataset. In addition, we added information, through a Boolean variable 'presence of an estuary', about the potential for each coastal segment to be significantly nourished by river sediments. This information is derived from the hydrographical network (source BD Carthage, French Geographical Institute (IGN)) considering that the main rivers are those that bring a significant amount of sediments to the coast. In practice, every coastal segment co-located with a river mouth was considered as significantly nourished by river sediments. This does not take into account alongshore sedimentary transport, that is, the capacity of a segment to be supplied with sediments from adjacent segments.

3.2.4. Cyclonic and seasonal waves and swells

The exposure to energetic waves is based on the modelling of the different types of waves affecting La Reunion (Lecacheux et al., 2012): the island is exposed to three main wave regimes — trade waves, southern swells and cyclonic waves. Trade waves are generated by trade winds (persistent planetary-scale surface winds). They come from the east-south-east in the Southern hemisphere and cause alongshore

sedimentary transport from the south-east to the north-west of the island. Southern swells and cyclonic waves are highly energetic and capable of triggering erosion, the first affecting primarily the south-western part of the island and the second the north-eastern part. Considering that this last process is the most important for shoreline changes, we split the island coasts in three categories: "mainly exposed to cyclonic waves", "mainly exposed to southern swells" and "protected by coral reefs" (Fig. 1). This is acknowledged as an oversimplification of reality, for example, coral reef hydrodynamics are particularly complex (see e.g. Storlazzi et al., 2011). The resulting map can be viewed as a first order approximation, which meets the requirements for use in BN, that is the mutual exclusivity and collective exhaustivity of the variables' states (Heckerman, 1997).

3.2.5. Tides

In La Réunion, the tidal regime is semi-diurnal and asymmetrical. It is microtidal since the tidal range varies between 0.1 m (neaps) and 0.9 m (springs) (Bourmaud et al., 2005). The tidal range is uniform all around the island and it cannot explain the heterogeneity of the observed shoreline evolution. Consequently, this factor is not included in our Bayesian model which is focused on shoreline mobility.

3.2.6. Relative sea-level rise at the coast

Relative sea-level rise at the coast can be viewed as the sum of two components: the climatic-component of sea-level rise (global mean sea-level rise plus the regional variability) and regional to local coastal ground motions. Although no tide gauge with a sufficiently long timeseries is available for the island, the multidecadal rates of sea-level rise can be assessed by evaluating each of these components separately.

The climatic component of sea-level rise can be assessed from satellite altimetry available for the two recent decades and for longer time periods (1950–2010) from a reconstruction of past sea-level changes (Fig. 2). In the southern zone of La Réunion, satellite altimetry indicates a rise of 7.5 ± 1.5 mm/yr from 1993 to 2010, whereas a sea-level reconstruction based on Meyssignac et al. (2012) indicates that the rise from 1950 to 2010 has been 1.2 ± 0.65 mm/yr (Palanisamy et al., 2014). In addition, since the size of La Réunion island does not exceed a width of 80 km, the climatic component of sea-level change is not expected to be significantly different around the island. To summarize, these results indicate that La Réunion island has been affected by a uniform climatic rise in sea-level, which has probably not been linear in time (Fig. 2).

To investigate whether the local vertical ground motions in La Réunion are significant and could induce variable relative sea-level rise rates along the coast, data from levelling measurements were used. The precision of this geodetic technique enables one to highlight relative ground motions up to a few millimetres. Using data obtained from surveys undertaken on the island by the French Geographical Institute (IGN) in 1958 and 1989 along the main roads of La Réunion, we compared the cumulative observed differences in height along the coast between these two operations spaced in time and on the same landmarks. The resulting data provide an estimate of the differential vertical ground motions along the coast between 1958 and 1989, up to an additive constant. In other words, additional information on ground deformations between 1958 and 1989 is needed in at least one location to estimate vertical ground motions along the entire levelling path. Here, the reference point for the calculation of the cumulative observed differences in height is chosen at a permanent GPS established by IGN near the point AM-64 (church of St-Leu,) and located close to the levelling path. This enables one to evaluate this constant. The data indicate daily vertical displacement oscillating around 0 cm (http://rgp.ign.fr/STATIONS/#SLEU). Although this time series is short (4 years), it suggests that this area is relatively stable. Therefore, we make the hypothesis that the landmark AM-64 is stable between the two dates.

The data presented above enable one to provide a first estimate of relative sea-level rise rates along the coasts of La Réunion island. These results are presented in detail in Section 4.1, and this information is integrated into the coastal dataset (Fig. 1). Importantly, it is hypothesized that the rates of vertical ground motions are linear, and that no more local ground motions are affecting coastal areas.

3.3. The Bayesian network for La Réunion

The structure of the Bayesian network applied to the coastal database of La Réunion is represented in Fig. 3. This graph has been elaborated by starting from the one of Gutierrez et al. (2011) and considering the necessary adaptations to the particular case of La Réunion. The final graph therefore reflects a simplified understanding of the functioning of the coastal systems, where 5 explanatory variables are considered: geomorphic setting, presence of an estuary, presence of anthropic structures, exposure to energetic waves and the rate of relative sea-level rise. The influence of one variable on another is represented by an arrow. For example, human works can disrupt the natural sedimentary transfer processes and therefore influence shoreline evolution. Also, since coral reefs are usually non-existent in front of river mouths, there is a direct influence of the variable "presence of an estuary" on the "exposure to energetic waves" variable. It should be mentioned that BNs can work with qualitative or quantitative variables. In the last case, it is possible either to discretize the data in bins or to keep the variables continuous using appropriate methods to compute the parameters (Aguilera et al., 2011). Here, all the variables in the database are originally discrete and each is resolved in several qualitative states or bins. The number of bins and their descriptions for the 5 variables are summarized in Table 1.

The BNT toolbox for Matlab (Murphy, 2001; https://code.google.com/p/bnt/) is used to construct the BN. Some routines have been modified to account for the different length of each coastal segment (see Section 2).

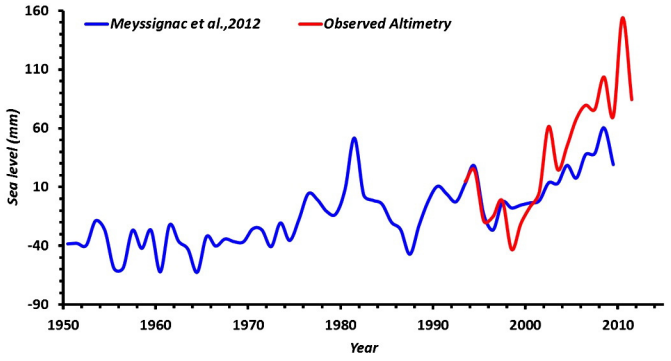

Fig. 2. Sea-level changes around La Réunion island in a geocentric framework (i.e. not taking into account ground motions). Red: observations from satellite altimetry. Blue: reconstruction of past sea-level changes due to climate change and variability (Meyssignac et al., 2012; Palanisamy et al., 2014).

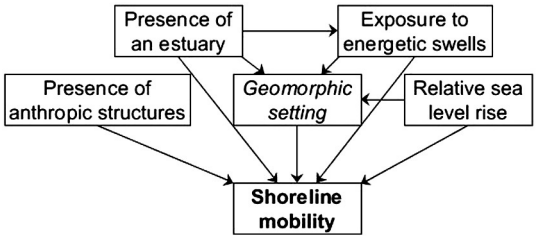

Fig. 3. Structure of the Bayesian network set up for the coastal database at La Réunion. Three types of variable are distinguished. Shoreline mobility is the response variable (in bold). Geomorphic setting is the inherent characteristic of the coastal segment (in italics) while the 4 remaining variables are driving forces of shoreline mobility.

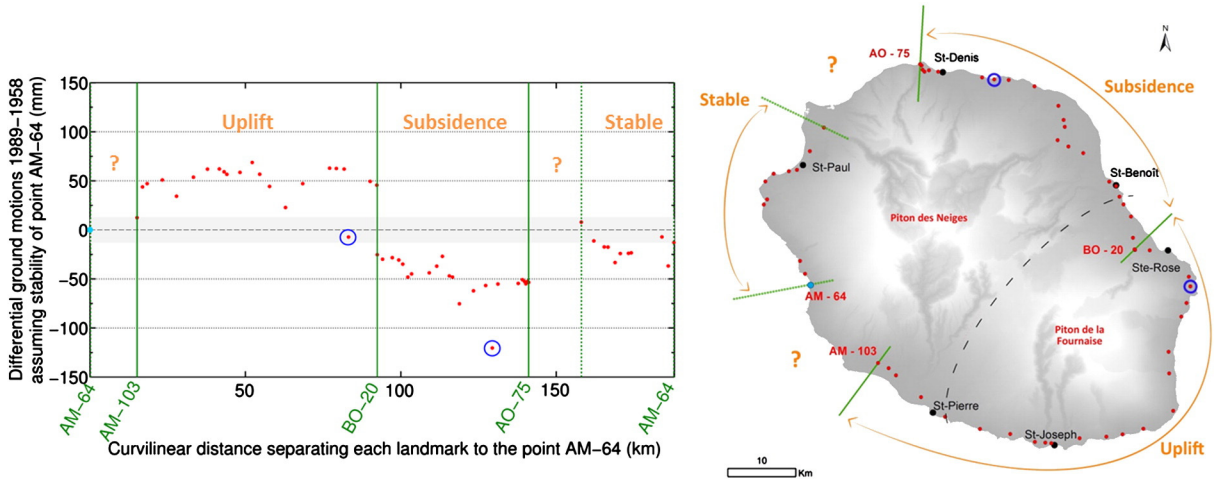

Fig. 4. Differential ground motions between 1989 and 1958 estimated from the analysis of two campaigns of levelling measurements. Ground motions are known up to a constant assumed to be equal to zero at point AM-64. The curvilinear distance from point AM-64 (abscissa axis) goes counter-clockwise around the island. Two points are circled in blue, pointing out probable displacements of landmarks between the two dates. The green lines indicate the boundaries between areas affected by different vertical ground motions. The question marks indicate where these boundaries cannot be placed accurately because no common landmarks are available in these areas between the two levelling surveys. The grey area on the left part of the figure represents the measurement uncertainty (maximum closure difference of 13 mm approximately, obtained for the 1958 series) and the range of non-significant results. Raw levelling data and the computation of raw height differences were produced by IGN (Lavoué, 2013).

4. Results

4.1. Relative sea-level rise along the coasts of La Réunion island

Fig. 4 shows the vertical ground motions along the coast, as obtained by comparing the differential vertical ground motions for the 57 common landmarks of the 1989 and 1958 levelling surveys. Despite some abrupt differences, probably due to the displacement of landmarks (circled in blue in Fig. 4), it appears clearly that the vertical ground motions are not homogeneous across the island between these two dates. Three areas can be distinguished, one with an uplift trend (south and southeast of the island), one which tends to subside (north and northeast of the island) and a "stable" or slightly subsiding area (western part of the island).

These results are rather consistent with intuition since it highlights uplift of the active volcanic system of the island. For the following, an assumption is made that these observed vertical ground motions are representative of a long-term general tendency. The rates of the vertical ground motions are therefore in the range of ± 1 to 2 mm/year. These rates are in the same order of magnitude as global present-day sea-level rise. Combining local-scale ground motions with the climatic component of the total relative sea-level rise signal, we conclude that the relative sea-level rise is significantly affected by vertical ground motions along the coast. Hence the description of the "relative sea-level rise velocity" variable in three states: "high" (corresponding to the subsiding area), "medium" (stable area) and "low" (uplifting area) (Fig. 1 and Table 1).

4.2. Evaluating the BN performance

This section examines the performance of the BN network of Fig. 3, whose parameters are calculated from the observations (Fig. 1). It corresponds to the last two steps of the method described in part 2.

Using all 5 variables, a predictive model based on our BN correctly reproduces the observed mobility for about 83% of the shoreline length (compared to 58% in the random case, see Appendix A). More precisely,

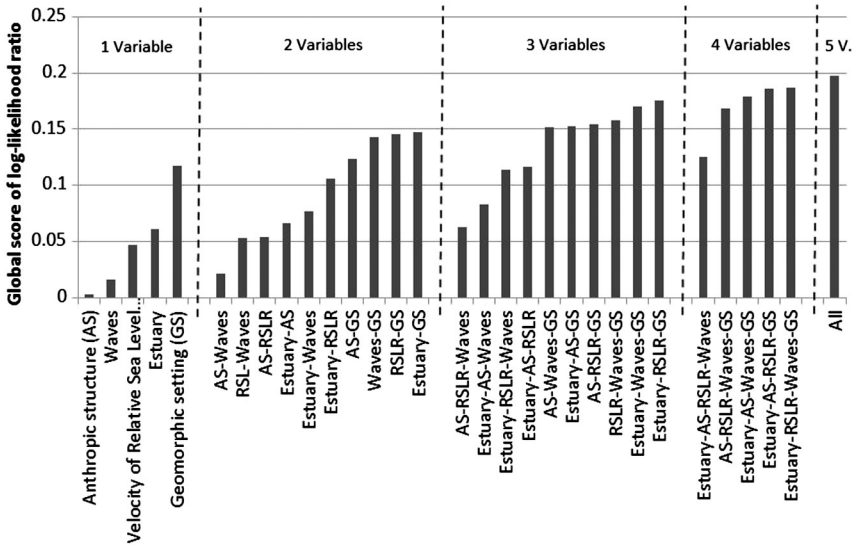

Fig. 5. Global log-likelihood ratio scores obtained for different BNs using 1 to 5 explanatory variables. (Theoretical boundaries: $LR_{min} = 0$; $LR_{max} = 0.38$, see Appendix B).

87% of stable shoreline, 82% of eroding shoreline and 73% of accreting shoreline are correctly predicted. The global log-likelihood ratio *LR* reaches almost 0.2 (Fig. 5).

In order to quantify the strength of the relationships between each explanatory variable and shoreline mobility and to evaluate the relative importance of each variable with respect to shoreline mobility, the global *LR* of the complete model is compared with simpler models using 1 to 5 variables (Fig. 5). For a BN with two variables (shoreline mobility and one explanatory variable), the highest score is obtained when considering the geomorphic setting (GS). For a BN with more variables, any combination of variables including GS systematically leads to the highest values of *LR*. The second most important variable is the presence of estuaries in the vicinity of coastal segments, followed by the rate of relative sea-level rise (RSLR). The last 2 variables, namely the presence of anthropic structures (AS) and the exposure to energetic waves (Waves), have a minor role in the overall performance of the BN, whatever the combination of variables.

To go deeper into the analysis of BN performance, we then identify the states of the variables that are related to successful predictions of accretion, stability or erosion. Fig. 6 shows the characteristics of successful retrospective predictions of the complete model: they correspond to cases where the black squares (correct predictions) take relatively high values while the corresponding diamonds (incorrect predictions) take significantly lower values. Accretion (third row) is found to be successfully predicted for a large proportion of the shoreline located near estuaries. Stability (second row) is correctly predicted for a significant proportion of the shoreline where anthropic structures are present, it is protected by reefs, the geomorphic setting is 'cliff behind shingle bar', 'micro-cliff behind shingle bar', 'shingle beach', 'sand beach' or 'low rocky coast', or the rate of relative sea-level rise is medium to high. Last, erosion (first row) is successfully predicted for a large proportion of the shoreline where it is exposed to southern swell, the geomorphic setting is 'cliff', 'low rocky coast' or the rate of relative sea-level rise is the lowest. The high percentage of shoreline being 'micro-cliff behind sand bar' (bin 5)

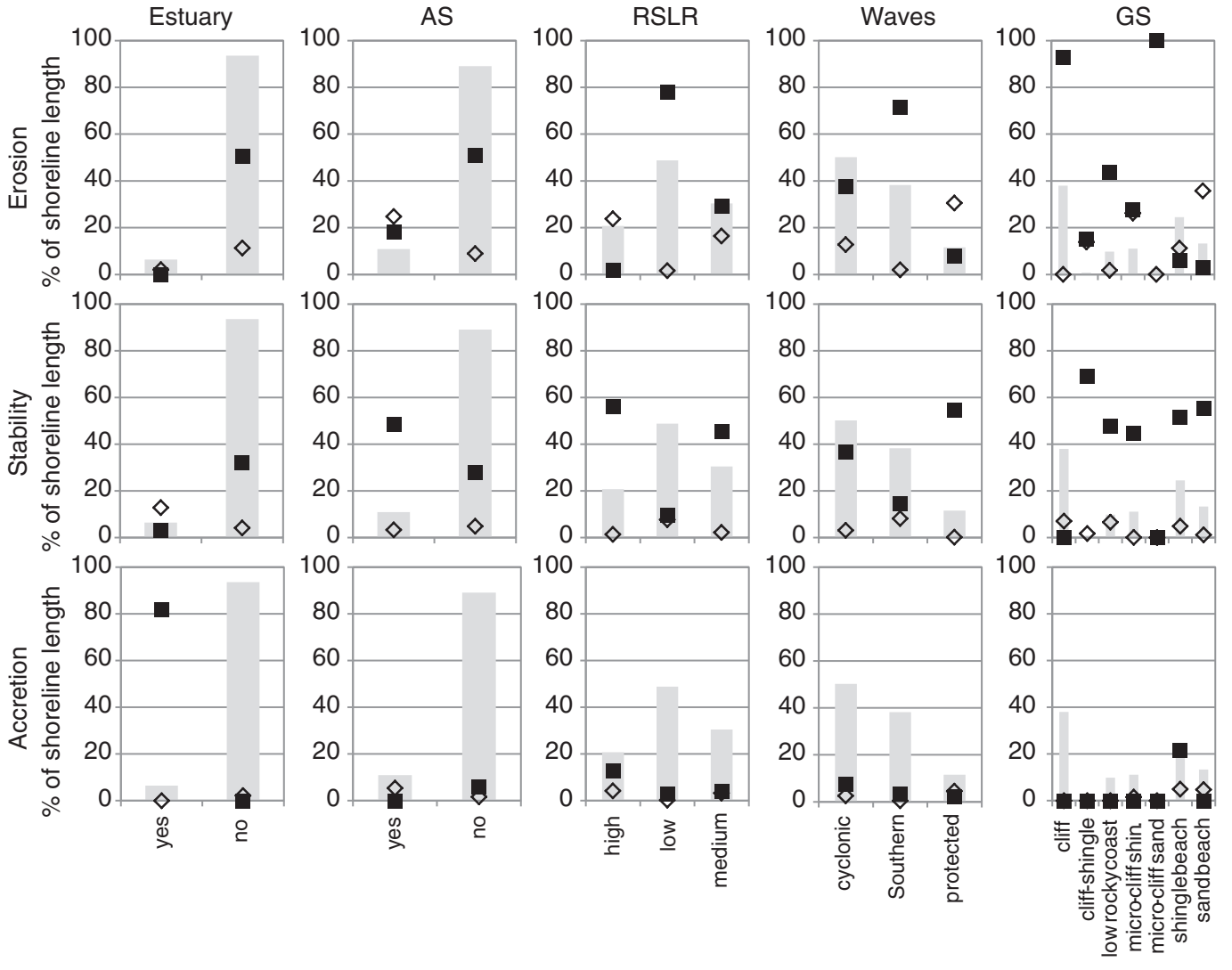

Fig. 6. Characteristics of successful predictions: black squares (resp. diamonds) represent the percentage of shoreline length falling in a given variable state, observed in erosion (first row), stability (second row) or accretion (third row), and correctly (resp. incorrectly) predicted. For black squares, that percentage is obtained as the shoreline length in erosion, stability or accretion correctly predicted where a given variable (column) is in a specific state divided by the total length with that variable state in the dataset and multiplied by 100. For diamonds, it is obtained as the shoreline length in erosion, stability or accretion incorrectly predicted where a given variable (column) is in a specific state divided by the total length with that variable state in the dataset and multiplied by 100. Therefore, the sum of the three black squares and the three diamonds for each variable state equals 100. For example, in the bottom left graph, the highest black square specifies the cumulative length of coastal segments correctly predicted in accretion divided by the cumulative length of coastal segments having an estuary in their neighbourhood in the entire database (then multiplied by 100). Similarly, the corresponding diamond is the cumulative length of coastal segments observed in accretion but wrongly predicted, divided by the cumulative length of coastal segments having an estuary in their neighbourhood in the entire dataset (then multiplied by 100). The grey bars in each graph show the percentage of shoreline length for each variable state in the initial dataset (prior probability distributions).

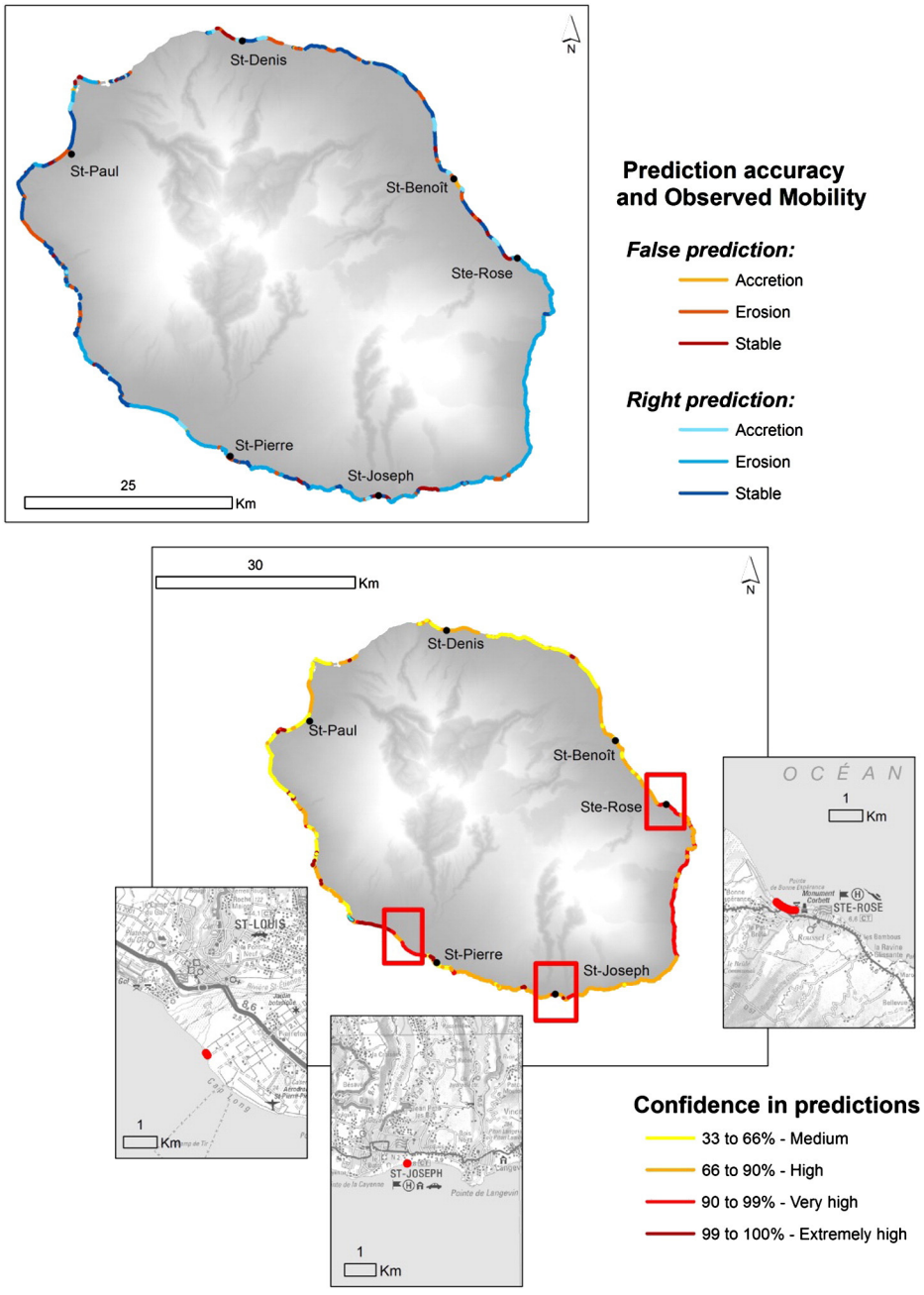

Fig. 7. Spatial variability of the predictive model outcome. Top: false and correct predictions and observed shoreline mobility for each coastal segment. Bottom: map of the confidence in the predictions, i.e. the probability of the predicted outcome. The red rectangles identify 3 segments that are incorrectly predicted with 'very high' confidence. Predictions in the northern part of the island are more uncertain than in the southern part. This indicates characteristics of coastal segments in the north with relatively wider probability distributions of shoreline mobility than in the south.

correctly predicted in erosion comes from the low representation of that variable category in the dataset (2.5% of the whole shoreline). The presence of anthropic structures does not inform much about erosion (black square and diamond taking similar values) but seems to be related to shoreline stability.

All the strong links found between each explanatory variable and shoreline mobility, as shown in Fig. 6, are consistent with an intuitive analysis, except for the rate of relative sea-level rise: for more than 55% of the shoreline where RSLR velocity is the highest, shoreline mobility is correctly predicted as stable, whereas for about 80% of the shoreline whose RSLR velocity is the lowest, shoreline mobility is correctly predicted in erosion. In other words, erosion is more frequent when the RSLR velocity is the lowest. This paradoxical behaviour of RSLR in the model is discussed in detail in Section 5.2.

Because of the counter-intuitive behaviour of the variable RSLR velocity, the next results are obtained using only the four other variables.

4.3. Performance with 4 variables

The global *LR* score of the BN using 4 variables (geomorphic setting, presence of estuary, presence of anthropic structures and exposure to energetic waves) is 0.18 (Fig. 5) and the proportion of the shoreline whose observed mobility is correctly predicted is 81%. More precisely, 85% of stable shoreline, 79% of eroding shoreline and 73% of accreting shoreline are correctly predicted. Fig. 7 (top) shows the locations where the retrospective predictions are correct or not.

Fig. 7 (bottom) maps the probability of the most likely outcome, an indicator which can be interpreted as the confidence in the

retrospective prediction. This map can be used to identify areas where there is a high level of uncertainties or great confidence in the outcome prediction (Gutierrez et al., 2011) which is useful to target where the BN needs improvements. Globally, more than 67% of the shoreline is correctly predicted with a 'high' confidence level or above (probability of the most likely outcome greater than 0.66) and almost 23% of the shoreline is correctly predicted with a 'very high' confidence level or above (probability of the most likely outcome greater than 0.9). By comparing Fig. 7 (top) and (bottom), we can also identify areas where there is great confidence in the outcome while the prediction is wrong. Only 3 of these particular sites are found falling within the 'very high' category, they are identified by red rectangles in Fig. 7 (bottom).

5. Discussion

5.1. Interpretation of BN results in terms of physical processes

Section 4.2 showed that geomorphic setting is the most important variable for understanding shoreline mobility on La Réunion. This is due to the fact that in the dataset, some well represented categories of GS are strongly linked to specific shoreline mobility. For example, 93% of cliffs in La Réunion are observed in erosion and cliffs are the main geomorphic settings around the island (38% of the shoreline). The presence of an estuary in the vicinity of a segment is the second most important variable for understanding shoreline mobility. In particular, it is the only characteristic identified to successfully predict accretion (see Section 4.2 and Fig. 6). This can be easily interpreted as accreting segments around the island are often subjected to the influence of river sediment supply: 73% of accreting shoreline has an estuary in its neighbourhood.

Stable and eroding coasts are better predicted by the BN than accreting shorelines, but the result for the latter category is still satisfying (73%, see Section 4.3). In fact, 100% of correctly predicted accreting shoreline has an estuary nearby which indicates that the remaining 27% of accreting shoreline has no estuary and is systematically mispredicted. That might be the result of a combination of factors including the relative scarcity of data for the accretion category (only 7% of the coast is accreting), which may prevent the BN from accurately identifying combinations of variables leading to accretion, and the incompleteness of the BN structure which does not take into account processes of sedimentary transport along the coast.

Alongshore sedimentary transport processes are generated by currents induced mainly by trade waves (see Section 3.2.4). They redistribute fine and coarse materials of marine or terrestrial origin (cliff and riverine sediments) along the coast from the south-east to the north-west. Although it is difficult to quantify the effect of these processes on shoreline mobility, there is evidence of their influence on local coastal evolution. For example, a natural rocky outcrop at La Pointe du Bourbier acts as a wall, stopping the coastal drift and accumulating sediments upstream. As a result, the coastal segment located immediately upstream of the outcrop is accreting (Fig. 8). Anthropic structures implanted directly on the shoreline, such as harbours, marinas or jetties, also highlight the importance of alongshore sedimentary transport when they disrupt it. A case in point is the jetty of Le Butor at Saint-Benoît where sediments accumulate updrift of the structure whereas erosion is observed downdrift (Fig. 8). These examples attest to the significant role played by alongshore transport in local sedimentary budgets and coastal evolution. As our BN model fails to take it into account, we might expect some mispredictions in the evaluation of BN performance in these cases.

It was noted in Section 4.2 and Fig. 5 that the presence of anthropic structures is the variable which has the weakest explanatory power with respect to shoreline mobility. However, stability seems to be successfully predicted when such structures are present (Fig. 6). This feature is then probably due to spatial correlation with other variables having higher explanatory power. Indeed, anthropic structures are mostly located on the west coast, where sandy beaches can be found as well as protecting reefs. These two variables' states are related to successful stability predictions and the corresponding variables (Geomorphic Setting and Waves) have stronger links with respect to shoreline mobility. Therefore, even if locally there is evidence of the direct influence of human interventions on shoreline mobility, other variables seem to dominate and control shoreline mobility at the scale of the island. It is worth noting that the influence of a human works located on a given coastal segment on an adjacent segment is not taken into account in our model. That might also explain the relatively weak link between the variables Anthropic Structures and Shoreline

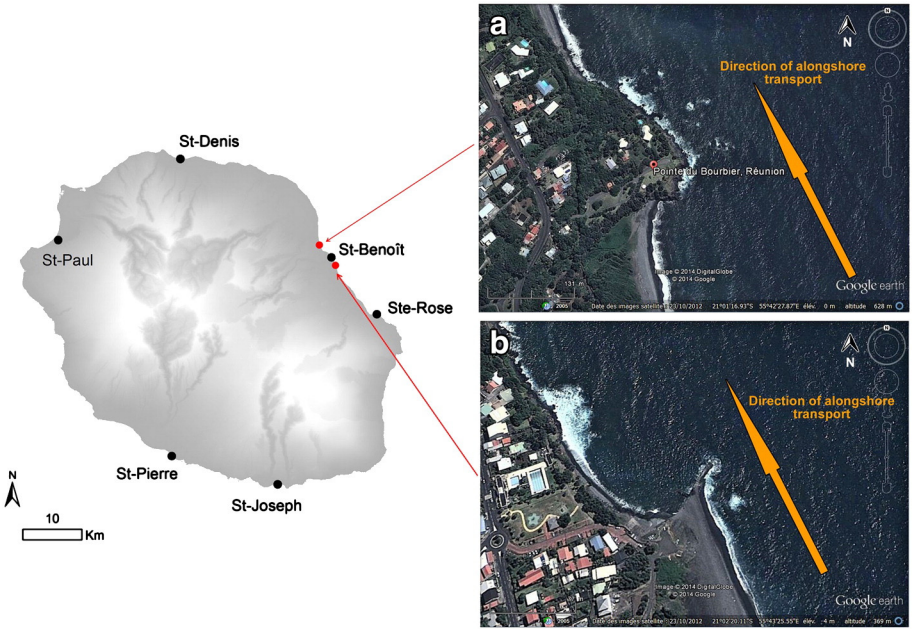

Fig. 8. Satellite views and localisation of a) the natural rocky outcrop at La Pointe du Bourbier, and b) the jetty of Le Butor at Saint-Benoît. The direction of the alongshore sedimentary transport is indicated by an orange arrow.

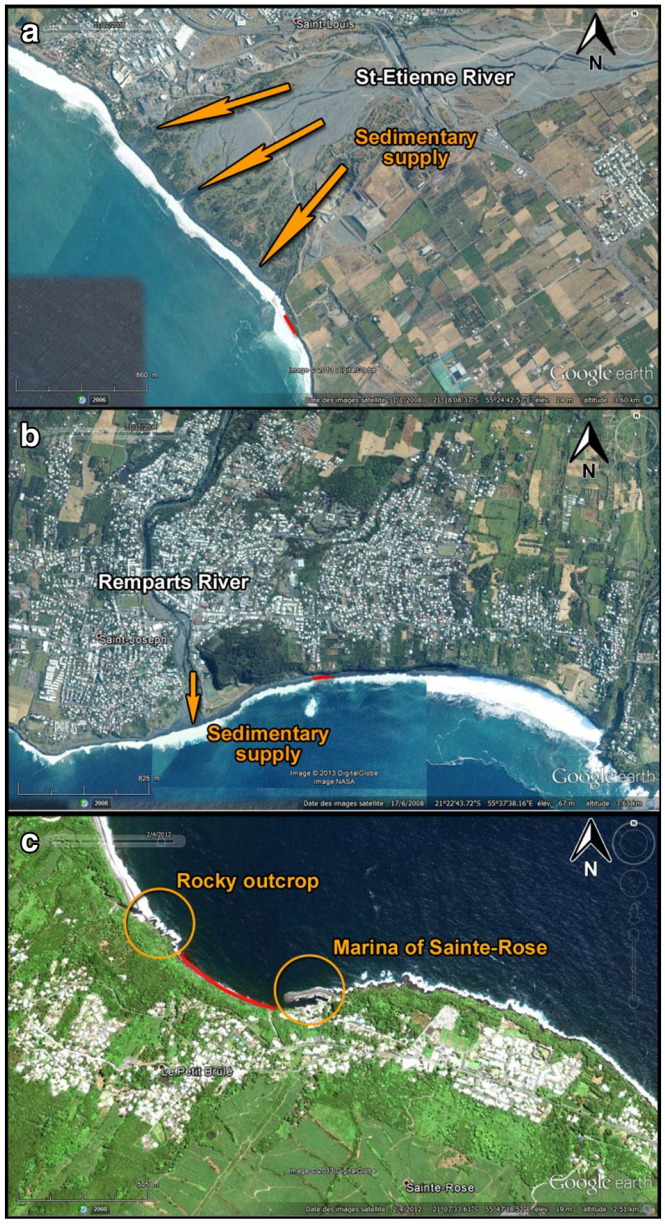

Fig. 9. Satellite views of the 3 zones identified in Fig. 6 (bottom). The coastal segments represented in red are wrongly predicted with great confidence. They are very specific and their mobility differs from the most common behaviour of similar segments. a) Segment located near Saint-Louis. b) Segment located near Saint-Joseph. c) Segment located near Sainte-Rose.

Mobility if the main impact of a structure is not felt in its immediate vicinity (i.e. the same segment) but relatively far from it (i.e. other segments).

Mispredicted areas with a high confidence level in the predicted outcome (Fig. 7) correspond to particular sites that differ from the common behaviour. Indeed, our predictive model constructed from the BN only reproduces the most common or probable shoreline mobility for a given set of characteristics. For example, Fig. 9 shows a satellite view of each of the 3 segments identified in Section 4.2, which are incorrectly predicted with great confidence. Looking more closely at these sites aids understanding as to why they are specific:

- the coastal segment near Saint-Louis (Fig. 9a) is predicted as being in erosion but is observed in accretion. The satellite picture indicates this segment is very close to the mouth of the Saint-Etienne River but not directly in front of it so that the 'Estuary' variable is set to 'No'. However, the influence of the river as a sediment supplier to the coast is likely to be felt by segments away from the mouth due to alongshore sedimentary transport. This might be the cause of the misprediction and it underscores a weakness of the BN, already mentioned above, which fails to take into account alongshore sedimentary transport processes.
- the coastal segment near Saint-Joseph (Fig. 9b) is predicted in erosion but is observed as stable. Its location is in a cove near the mouth of the Remparts River so that, similar to the previous segment, sediment supply by the Remparts river (Garcin et al., 2005) might compensate the erosive trend of that segment type and account for the observed stability of the segment.
- the coastal segment near Sainte-Rose (Fig. 9c) is predicted in erosion while observed as stable. It is located in a cove between a rocky outcrop and the marina of Sainte-Rose. This particular configuration may retain sediments in the cove and protects the shoreline from the impact of waves coming from south to south-east. This could explain the observed relative stability.

These examples show that the retrospective predictions of the BN, whether successful or not, can often be interpreted in terms of physical processes. They also demonstrate that BN results must be interpreted with care to get insight into the role of each variable. This point is discussed more on the particular case of the RSLR velocity variable in the next section.

This analysis at regional scale suggests priorities for future studies focusing on the most significant factors driving shoreline changes in La Réunion, in particular the role of sediment inputs by rivers and their remobilization through coastal alongshore processes, and of different coastal geomorphic features (e.g. stratigraphy, lithology, etc.…), particularly for coastal systems with the most uncertain predictions (e.g. beaches, see Fig. 7). While the last is acknowledged important by many studies (Trenhaile, 1987; Sunamura, 1992; Finkl, 2004; Hampton and Griggs, 2004; Idier et al., 2013; Loureiro et al., 2013), the first often remains difficult to quantify (e.g. Dearing et al., 2006).

5.2. Role of differing rates of sea-level rise in the model and physical sense

In this section, we discuss the counter-intuitive behaviour of the RSLR velocity variable as related to shoreline mobility and described in Section 4.2.

The RSLR velocity is the third most important variable in the 5 variables BN (Fig. 5) but it behaves in a paradoxical way (Fig. 6). This is confirmed in a more general manner looking at the marginal probability distribution of shoreline mobility given RSLR velocity, all the other variables being unknown (Table 2): coastal segments affected by faster rise of sea-level have only 29% chance to be in erosion, whereas those facing a slow rising sea-level have 79% chance to be in erosion. If we just consider beaches, which are considered more sensitive to sea-level rise, we again find no consistency between RSLR and shoreline mobility (Tables 3 and 4): the probability of stability dominates whatever the RSLR velocity for shingle beaches and the probability of erosion is even lower than the probability of accretion; for sand beaches, the probability of erosion is very high (87%) when they face a slow rising level. Should the RSLR velocity variable play a significant role in the shoreline

Table 2
Probability distribution of shoreline mobility given RSLR (5 variables BN). Values are obtained using the junction tree algorithm (Murphy, 2001).

	Shoreline mobility		
RSLR	Stability	Erosion	Accretion
High	0.59	0.29	0.12
Low	0.17	0.79	0.04
Medium	0.51	0.41	0.08

Table 3
Probability distribution of shingle beaches mobility given RSLR (5 variables BN). Values are obtained using the junction tree algorithm (Murphy, 2001).

	Shoreline mobility of shingle beaches		
RSLR	Stability	Erosion	Accretion
High	0.63	0.17	0.20
Low	0.68	0.04	0.28
Medium	0.63	0.15	0.22

mobility, cases where erosion is observed should be correlated with a faster rate of sea-level rise rather than a slow rising level (Zhang et al., 2004; Gutierrez et al., 2011; Romine et al., 2013; Shearman et al., 2013). In the case of La Réunion island, differing rates of relative sea-level rise have therefore no consistent perceivable impacts on shoreline mobility, suggesting that other processes dominate (see e.g. Stive, 2004; Webb and Kench, 2010; Ford, 2013; Yates et al., 2013). Noteworthy is the fact that RSLR is unlikely to impact the coastal geomorphology (recall arrows in Fig. 3) significantly here. Its role is indeed counter-intuitive. For example, Fig. 1 shows that cliffs are more frequent where the RSLR velocity is the lowest. This suggests there is no causal link between RSLR and cliffs. Instead, RLSR seems to serve as proxy for the uplift rate since uplift is the mechanism which creates elevated landforms such as cliffs.

The part of the island with an uplift trend is localised south and south-east and corresponds well with the influence zone of the active volcano Piton de la Fournaise (indicated with a black dashed line in Fig. 3). In fact, all the coastal landforms in this area are remnants, more or less recent, of the volcanic activity of the Piton de la Fournaise. In our BN, the volcanic activity is partially embedded in the GS variable, as cliffs and low rocky coasts are mainly made of more or less consolidated volcanic materials, and in the RSLR variable, integrating the uplift rate. Notwithstanding the limitations of the data used for assessing relative sea-level rise at the coast (see Section 3.2.6), we can interpret the obtained results if we consider that the dominant mode of coastal changes remains inseparable from the volcanic origin of the island: schematically, the volcanic products first reach the sea directly or after remobilization by rainfall and then are permanently undergoing coastal erosion. Our results suggest that the different rates of RSLR have a minor role compared to these processes. The high value of P(SM = erosion| RSLR = low) could just be due to spatial correlation between eroded landforms and uplifting coasts, both features being a consequence of the internal and external geodynamic mechanisms (volcanism (eruptions and uplift), erosion) that dominate the coastal geomorphic changes of the island. This illustrates once more that an in-depth analysis of BN results is required to avoid drawing wrong conclusions.

While this interpretation seems consistent, it would be important to test if coastal ground motions are linear in time or not. A third levelling campaign undertaken in 2007 by IGN is available but cannot be interpreted in terms of coastal ground motions because of data gaps. Delacourt et al. (2009) used InSAR data to provide information on vertical ground motions due to volcanic activity and landslides in La Réunion, but lack of coherence in the interferograms prevents the usage of this technique in the coastal zones. Finally, the recently installed permanent GPS could provide insight to this issue, but only at specific locations. This case study of La Réunion illustrates the fact that the spatial and temporal variability of relative sea-level changes along the coasts are often unknown and difficult to monitor, but they deserve specific attention since they are often not negligible compared to multidecadal sea-level rise.

Table 4
Probability distribution of sand beaches mobility given RSLR (5 variables BN). It should be considered that most of sand beaches are located on the western side of the island. Values are obtained using the junction tree algorithm (Murphy, 2001).

	Shoreline mobility of sand beaches		
RSLR	Stability	Erosion	Accretion
High	–	–	–
Low	0.12	0.87	0.01
Medium	0.60	0.35	0.05

6. Conclusions

While the BN method used in this study is not new, its application to La Réunion island provides different insight into coastal processes than previous applications. First, it is shown that, when building the database, rates of relative sea-level rise are not homogeneous at the scale of the island: the south-eastern part of the island uplifted from 1958 to 1989, the western part remained stable and the north-western part subsided. However, our results show that these differing rates of relative sea-level change did not significantly affect shoreline mobility. Instead, the results suggest that decadal coastal evolution in the island remains largely controlled by three major geomorphic processes ((i) coastal and (ii) inland sediment transport; (iii) volcanism, which provides erodible materials and generates ground motions) and by local geomorphic settings. This finding thus suggests that relative sea-level rise being an important cause for observed different rates of shoreline erosion (Zhang et al., 2004; Gutierrez et al., 2011) is not generally applicable to every other coastal site.

This study confirms the considerable potential for Bayesian networks to explore coastal databases and gain insight into coastal processes and factors causing shoreline changes, including sea-level changes. However, this work also identifies several difficulties in using BNs for exploring coastal datasets:

- First, an initial coastal dataset of high quality is a necessary prerequisite to perform any interpretation of shoreline change causes. To undertake this study, it was necessary to reprocess and complete the initial dataset. Our first tests enabled us to detect and correct small inconsistencies in the initial database, which would have been difficult to notice otherwise due to the large amount of coastal data (e.g. inaccurate location of fringing reefs, etc.).
- Secondly, it is necessary to pay attention to the representativeness of the dataset: a BN can operate even with very few data but at the cost of a lower accuracy in the outcomes, as it has been illustrated with the category 'micro-cliff behind sand bar' in Fig. 6. It is tempting to add other variables to the network or to consider more categories in each variable in order to reduce the uncertainties in the model outcome (Fig. 7). However, such an approach is likely to result in too few data available for each combination of variables, leading to an artificially deterministic BN. Therefore, it is important to find a compromise between improving the description of the network structure and keeping sufficient samples of data for each case considered during the learning phase.
- A third limitation concerns the physical meaning of the network structure: unlike many applications of Bayesian networks, the graph used here (Fig. 3) is not an accurate representation of the reality. On the contrary, it remains simplified scheme of coastal systems evolution. In any application of this approach, it is important to highlight that the graph will significantly impact results as it acts as previous knowledge but also that it inherits the initial dataset ontology, at least partly.
- Finally, the BN approach is useful to highlight particularly strong relationships between variables, but it does not provide us with the nature of those relationships. This last point is illustrated by the role of differing rates of relative sea-level rise in our study and the fact that this variable serves as a proxy for another causal factor (the uplift rate).

Any application of this approach therefore requires systematic completion of BN results with an in-depth analysis of the data and of the processes taking place in these coastal sites.

The complexity of coastal system behaviours currently prevents their modelling purely based on physical concepts. In addition, there is a crucial need for public authorities to understand and manage coastal environments. Bayesian networks contribute to answering this need by improving our understanding of coastal evolution at decadal timescales. They could ultimately allow moving towards long-term predictions of future coastal environment evolution.

Acknowledgements

This work has been completed within the CECILE project (Coastal Environmental Changes: Impact of sea LEvel rise) supported by the French National Agency for Research (ANR) within its Planetary Environmental Changes (CEP) framework: convention n°ANR-09-CEP-001. We thank the regional office of BRGM at La Réunion island (S. Bès de Berc, E. Chateauminois, Y. de la Torre) for providing coastal data initially collected for the Region and DIREN and for their comments. We also thank IGN (S. Lavoué, A. Coulomb) for providing raw levelling data and A. Cazenave, B. Meyssignac, D. Raucoules and C. Mirgon for useful discussions. Last, we thank two anonymous reviewers as well as A.J. Plater for their comments which contributed to improve this paper.

Appendix A. Calculation of the percentage of shoreline length correctly reproduced in the random case

In order to evaluate the significance level of the model, it is necessary to compare the percentage of shoreline length correctly predicted to the one obtained with a completely randomized dataset (while respecting the prior probability distributions of all variables, i.e. the probability distributions of the variables calculated from their frequencies of appearance in the database), thus removing any dependency between variables. In that case, Eq. (2) becomes:

$$SM_{pred} = arg\,\max_i \left(P\left(SM^i \middle| \tilde{X}_j\right)\right) = arg\,\max_i \left(P\left(SM^i\right)\right) \quad (A.1)$$

As a result, whatever the coastal segment, the shoreline mobility state having the maximum prior probability is systematically predicted. We then deduce the percentage of shoreline length correctly predicted in the case of a completely randomized dataset as follows:

$$\%\ correct\ \ predictions = \max_i \left(P\left(SM^i\right)\right) \times 100 \quad (A.2)$$

In our dataset, the prior probability distribution of shoreline mobility is: P(erosion) = 0.58, P(accretion) = 0.07, P(stability) = 0.35. Therefore, the percentage of shoreline length correctly reproduced in the random case is 58%.

Appendix B. Calculation of the possible maximum and minimum theoretical values of the global log-likelihood ratio

The possible maximum theoretical *LR* can be computed directly from Eq. (4) by replacing $LR_{(k)}$ by its maximum theoretical value:

$$LR_{(k)} = \log\left(P\left(SM_{(k)} \middle| O_{(k)}\right)\right) - \log\left(P\left(SM_{(k)}\right)\right) = -\log\left(P\left(SM_{(k)}\right)\right) \quad (B.1)$$

From our dataset, we obtain $LR_{max} = 0.38$.

The minimum *LR* is computed when the entire dataset is randomized (but still following the prior probability distributions) thus removing any dependency between variables and is equal to 0.

References

Aguilera, P.A., Fernandez, A., Fernandez, R., Rumi, R., Salmeron, A., 2011. Bayesian networks in environmental modelling. Environ. Model Softw. 26 (12), 1376–1388.
Berger, J.O., 2000. Bayesian analysis: a look at today and thoughts of tomorrow. J. Am. Stat. Assoc. 95, 1269–1276.
Bourmaud, C.A.F., Abouïdane, A., Boissier, P., Leclère, L., Mirault, E., Pennober, G., 2005. Coastal and marine biodiversity of La Réunion. Indian J. Mar. Sci. 34 (1), 98–103.
Catenacci, M., Giupponi, C., 2013. Integrated assessment of sea-level rise adaptation strategies using a Bayesian decision network approach. Environ. Model Softw. 44, 87–100.
Cazenave, A., Le Cozannet, G., 2014. Sea level rise and its coastal impacts. Earths Futur. 2 (2), 15–34.
De La Torre, Y., 2004. Synthèse morphodynamique des littoraux de La Réunion, état des lieux et tendances d'évolution à l'échelle de l'île. Open file report BRGM/RP-53307-FR.
Dearing, J.A., Richmond, N., Plater, A.J., Wolf, J., Prandle, D., Coulthard, T.J., 2006. Modelling approaches for coastal simulation based on cellular automata: the need and potential. Philos. Trans. R. Soc. A Math. Phys. Eng. Sci. 364 (1841), 1051–1071.
Delacourt, C., Raucoules, D., Le Mouelic, S., Carnec, C., Feurer, D., Allemand, P., Cruchet, M., 2009. Observation of a large landslide on La Reunion Island using differential Sar Interferometry (JERS and Radarsat) and correlation of optical (Spot5 and aerial) images. Sensors 9 (1), 616–630.
Eurosion, 2004. Living with coastal erosion in Europe: sediment and space for sustainability. Part I: Major findings and policy recommendations of the EUROSION project.
Finkl, C.W., 2004. Coastal classification: systematic approaches to consider in the development of a comprehensive scheme. J. Coast. Res. 20 (1), 166–213.
Ford, M., 2013. Shoreline changes interpreted from multi-temporal aerial photographs and high resolution satellite images: Wotje Atoll, Marshall Islands. Remote Sens. Environ. 135, 130–140.
Garcin, M., Poisson, B., Pouget, R., 2005. High rate of geomorphological processes in a tropical area: the Remparts river case study (Réunion Island, Indian Ocean). Geomorphology 67 (3–4), 335–550.
Gillot, P.Y., Nativel, P., 1989. Eruptive history of the Piton de la Fournaise volcano, Réunion island, Indian Ocean. J. Volcanol. Geotherm. Res. 36, 53–65.
Gutierrez, B.T., Plant, N.G., Thieler, E.R., 2011. A Bayesian network to predict coastal vulnerability to sea level rise. J. Geophys. Res. Earth Surf. 116, 15.
Hampton, M.A., Griggs, G.B., 2004. Formation, evolution and stability of coastal cliffs — status and trends. USGS Professional Paper. 1683 (123 pp.).
Hapke, C., Plant, N., 2010. Predicting coastal cliff erosion using a Bayesian probabilistic model. Mar. Geol. 278 (1–4), 140–149.
Heckerman, D., 1997. Bayesian networks for data mining. Data Min. Knowl. Disc. 1, 79–119.
Idier, D., et al., 2013. Vulnerability of sandy coasts to climate variability. Clim. Res. 57 (1), 19–44.
Karunarathna, H., Reeve, D., 2007. Predicting morphodynamic response of a coastal plain estuary using a Boolean model. Proceedings of the 5th IAHR Symposium on River, Coastal and Estuarine Morphodynamics, Enschede, NL, 17–21 September 2007, pp. 1109–1115.
Karunarathna, H., Reeve, D., 2008. A Boolean approach to prediction of long-term evolution of estuary morphology. J. Coast. Res. 24 (2B), 51–61.
Lavoué, S., 2013. Comparaisons de nivellement sur le littoral réunionnais. CR/G 276, IGN, Servive de Géodésie et de Nivellement.
Le Cozannet, G., Garcin, M., Bulteau, T., Mirgon, C., Yates, M.L., Mendez, M., Baills, A., Idier, D., Oliveros, C., 2013. An AHP-derived method for mapping the physical vulnerability of coastal areas at regional scales. Nat. Hazards Earth Syst. Sci. 13 (5), 1209–1227.
Lecacheux, S., Pedreros, R., Le Cozannet, G., Thiebot, J., De La Torre, Y., Bulteau, T., 2012. A method to characterize the different extreme waves for islands exposed to various wave regimes: a case study devoted to Reunion Island. Nat. Hazards Earth Syst. Sci. 12 (7).
Loureiro, C., Ferreira, O., Cooper, J.A.G., 2013. Applicability of parametric beach morphodynamic state classification on embayed beaches. Mar. Geol. 346, 153–164.
Meyssignac, B., Becker, M., Llovel, W., Cazenave, A., 2012. An assessment of two-dimensional past sea level reconstructions over 1950–2009 based on tide-gauge data and different input sea level grids. Surv. Geophys. 33 (5), 945–972.
Murphy, K.P., 2001. The Bayes net toolbox for Matlab. Comput. Sci. Stat. 33 (2), 1024–1034.
Myllymäki, P., Silander, T., Tirri, H., Uronen, P., 2002. B-Course, a web-based tool for Bayesian and causal data analysis. Int. J. Artif. Intell. Tools 11 (3), 369–387.
Naïm, P., Wuillemin, P.-H., Leray, P., Pourret, O., Becker, A., 2007. Réseaux bayésiens. Eyrolles, Paris.
Palanisamy, H., Cazenave, A., Meyssignac, B., Soudarin, L., Woppelmann, G., Becker, M., 2014. Regional sea level variability, total relative sea level rise and its impacts on islands and coastal zones of Indian Ocean over the last sixty years. Glob. Planet. Chang. http://dx.doi.org/10.1016/j.gloplacha.2014.02.001.
Pearl, J., 1986. Fusion, propagation and structuring in belief networks. Artif. Intell. 29, 241–288.
Plant, N.G., Holland, K.T., 2011a. Prediction and assimilation of surf-zone processes using a Bayesian network part I: forward models. Coast. Eng. 58 (1), 119–130.
Plant, N.G., Holland, K.T., 2011b. Prediction and assimilation of surf-zone processes using a Bayesian network part II: inverse models. Coast. Eng. 58 (3), 256–266.
Plant, N.G., Stockdon, H.F., 2012. Probabilistic prediction of barrier-island response to hurricanes. J. Geophys. Res. Earth Surf. 117.
Quelennec, R.-E., Oliveros, C., Uhel, R., Devos, W., 1998. Corine: érosion côtière. Environmental and quality of life series. Office for Official Publications of the European Communities, Luxembourg (170 pp.).
Rocher, P., 1988. Contexte volcanique et structural de l'hydrothermalisme récent dans le massif du Piton des Neiges, île de La Réunion(PhD Thesis) Etude détaillée du Cirque de Salazie. Université de Paris Orsay.

Romine, B.M., Fletcher, C.H., Barbee, M.M., Anderson, T.R., Frazer, L.N., 2013. Are beach erosion rates and sea-level rise related in Hawaii? Glob. Planet. Chang. 108, 149–157.
Shearman, P., Bryan, J., Walsh, J.P., 2013. Trends in deltaic change over three decades in the Asia-Pacific Region. J. Coast. Res. 29 (5), 1169–1183.
Stive, M.J.F., 2004. How important is global warming for coastal erosion? An editorial comment. Clim. Chang. 64 (1–2).
Storlazzi, C.D., Elias, E., Field, M.E., Presto, M.K., 2011. Numerical modeling of the impact of sea-level rise on fringing coral reef hydrodynamics and sediment transport. Coral Reefs 30.
Sunamura, T., 1992. Geomorphology of Rocky Coasts. John Wiley and Sons, New York.
Thieler, E.R., Hammar-Klose, E.S., 1999. National assessment of coastal vulnerability to future sea-level rise: preliminary results for U.S. Atlantic Coast. U.S. Geol. Surv. Open File Report, Woods Hole, Massachusetts, 99-593.
Trenhaile, A.S., 1987. The Geomorphology of Rock Coasts. Oxford University Press, New York.
Uusitalo, L., 2007. Advantages and challenges of Bayesian networks in environmental modelling. Ecol. Model. 203, 312–318.
Webb, A.P., Kench, P.S., 2010. The dynamic response of reef islands to sea-level rise: evidence from multi-decadal analysis of island change in the Central Pacific. Glob. Planet. Chang. 72 (3), 234–246.
Yates, M.L., Le Cozannet, G., 2012. Brief communication 'Evaluating European Coastal Evolution using Bayesian Networks'. Nat. Hazards Earth Syst. Sci. 12 (4), 1173–1177.
Yates, M.L., Le Cozannet, G., Garcin, M., Salaï, E., Walker, P., 2013. Multidecadal atoll shoreline change on Manihi and Manuae, French Polynesia. J. Coast. Res. 29 (4), 870–882.
Yin, J., Yin, Z., Wang, J., Xu, S., 2012. National assessment of coastal vulnerability to sea-level rise for the Chinese coast. J. Coast. Conserv. 16 (1), 123–133.
Zhang, K.Q., Douglas, B.C., Leatherman, S.P., 2004. Global warming and coastal erosion. Clim. Chang. 64 (1–2).